Research Article

Huiying Zhang, Xiang Li, Wenjie Qian, Jianguo Zhu*, Beibei Chen*, Jin Yang, and Yu Xia

Characterization of mechanical properties of epoxy/nanohybrid composites by nanoindentation

https://doi.org/10.1515/ntrev-2020-0003
Received Aug 11, 2019; accepted Nov 05, 2019

Abstract: The carbon nanofibers and molybdenum disulfide (CNF-MoS_2) nanohybrid material was fabricated and incorporated into epoxy resin to form the nanocomposite coating. Firstly, microstructure observation shows that each CNF was uniformly wrapped up with MoS_2 nanosheets, and the nanohybrids were well dispersed in the coating. Then, nanoindentation experiments were carried out to explore the effect of the CNF-MoS_2 nanohybrids on the mechanical properties of the epoxy resin coating. The results demonstrate that elastic modulus, hardness and creep deformation resistance of the CNF-MoS_2 epoxy resin coating are greatly increased in comparison with both pure epoxy resin and MoS_2 epoxy resin coatings. Finally, the underlying mechanism of high-performance tribological behavior of the nanocomposites is analyzed accordingly. It can be concluded that the wrapped structure with MoS_2 sheets growing on the surface of CNF increases the contact area and reduces the friction coefficient of the composite coating, while the wear resistance of the nanocomposite coating is also greatly improved due to the superior high hardness of CNF.

Keywords: polymer-matrix composites (PMCs); nanohybrid; nanoindentation; mechanical properties

1 Introduction

Epoxy resin (EP) is one of the important types of high-performance thermosetting organic polymers and has been widely used as adhesives, coatings, and composite materials for a wide range of advanced applications such as in the field of aerospace, marine, and electronics, wear-resistant slide joints, tribological field, etc. Although epoxy resin has excellent adhesion strength, acid and alkali resistance, green environmental protection and so on, it is brittle in comparison with the metals and hence relatively low percentages of nanoparticles are incorporated into epoxy resin to improve its ductility as well as other mechanical properties [1, 2]. As one of the most eminent transition-metal dichalcogenides materials, molybdenum disulfide (MoS_2) has a unique structure, good thermal conductivity, excellent mechanical flexibility, and self-lubricating property. Thus, MoS_2 nanoparticles were commonly incorporated into epoxy resin to make epoxy coatings have better tribological properties under complex and harsh working conditions [3–5]. Recently, many researchers have focused on hybrids composed of MoS_2 and other components (*e.g.*, TiO_2 [6], reduced graphene oxide (rGO) [7–9], Fe_3O_4 nanoparticle [10], and carbon spheres [11], etc.), and these hybrids have much more reinforcing and lubricating effects than single MoS_2 [12]. It was reported that carbon nanofibers (CNFs) have extraordinary mechanical and electrical properties, high aspect ratio and low density, which make them a focus of research in the improvement of the polymer matrix characteristics [13, 14]. In addition, CNFs are easily available and have a relatively low price that makes them an excellent alternative to nanotubes (CNTs). It can be expected that CNFs and MoS_2 synergistically improve the tribological behavior of polymer composites, and it was reported that the incorporation of CNFs-MoS_2 hybrids had dramatic improvement of wear resistance with synthesis of CNFs-MoS_2 hybrids [15]. However, there remains a need for a quantitative study of the improving mechanism of tribological performance of the hybrid as a promising additive.

***Corresponding Author: Jianguo Zhu:** Faculty of Civil Engineering and Mechanics, Institute of Structure Health Monitoring, Jiangsu University, Jiangsu, China, 212013; Email: zhujg@ujs.edu.cn
***Corresponding Author: Beibei Chen:** School of Materials Science and Engineering, Institute for Advanced Materials, Jiangsu University, Jiangsu, China, 212013; Email: chenbb@ujs.edu.cn
Huiying Zhang, Wenjie Qian, Yu Xia: Faculty of Civil Engineering and Mechanics, Institute of Structure Health Monitoring, Jiangsu University, Jiangsu, China, 212013
Xiang Li, Jin Yang: School of Materials Science and Engineering, Institute for Advanced Materials, Jiangsu University, Jiangsu, China, 212013

Nanoindentation technology has been widely used as an advanced means for characterization of mechanical properties [16, 17]. Nanoindentation is a kind of indentation that continuously controls a certain indenter through high-resolution instruments so that it can be indented into the material at a certain rate and then unloaded. Mechanical properties of materials, such as Young's modulus and hardness, can be calculated according to the recorded data of load-displacement of the indenter during loading and unloading [18]. In 2000, Hodzic *et al.* analyzed the close relationship between the local mechanical properties and microstructure of epoxy/glass fiber composites by small load indentation experiments, especially the width of the interfacial phase between fiber and matrix can be obtained [19, 20]. In 2004, Shen and Liu made a systematic study on composite systems with nylon 6, nylon 66 and multi-walled carbon nanotubes (MWC-NT) as matrix, nano-clay, and fillers respectively using nanoindentation technology [21–24]. In 2007, Lee *et al.* used nanoindentation technique to measure the hardness and elastic modulus of the interfacial phase of fiber reinforced polymer composites [25]. In 2010, Melgarejo *et al.* studied the interaction between AlB_2 particles and Al matrix in Al/AlB_2 composites by nanoindentation method [26]. In 2011, Sánchez *et al.* measured the mechanical properties of carbon nanofibers/epoxy nanocomposites by nanoindentation method [27]. In 2017, Kavouras *et al.* used grid nanoindentation testing to explore the effect of local microstructure on the indentation induced damage of a fiber reinforced composite [28]. Additionally, creep of polymer and its composites is one of the significant mechanical behaviors that influence its service life, especially at the high-temperature environment. Tehrani *et al.* tested the creep properties of MWC-NT/epoxy nanocomposites using nanoindentation technique [29]. Hou *et al.* used an ultra-stable instrumented nanoindentation tester to study extremely long (30,000s) indentation creep of polymers [30]. Koumoulos *et al.* found that the introduction of nanodiamond (ND) particles can significantly reduce the creep of the material by nanoindentation method [31]. Kunal investigated the effects of dispersion technology and particle concentration on creep properties and other mechanical properties of epoxy matrix nanocomposites [32].

In this work, the mechanical properties of epoxy resin incorporated by CNFs-MoS_2 hybrids are experimentally investigated using nanoindentation technique, and the underlying mechanism of high-performance tribological behavior of the nanocomposites is provided. Firstly, epoxy resin composite coating was prepared by toughening epoxy resin with nanoparticles, and its microstructure and chemical composition were observed and measured. Secondly, the hardness, elastic modulus, and creep behavior of the epoxy resin composite coating modified by different nanoparticles were investigated by nanoindentation test. Lastly, the mechanical properties including elastic modulus and creep behavior were obtained and compared, followed by discussions on the relationship between microstructure and mechanical properties of the nanocomposites coating.

2 Nanoindentation test

Nanoindentation, also known as depth sensitive indentation, was first proposed by Oliver *et al.* in 1992. Oliver&Pharr method has been the most widely used method in calculating elastic modulus and hardness of materials. During the loading process of the nanoindentation test, elastic deformation occurs on the surface of the material at the beginning of loading. With the increase of the load, the plastic deformation of the material surface begins to appear and gradually increases, which leads to the nonlinear segment of the loading curve. After the maximum load, the elastic deformation of the material surface will gradually disappear with unloading, and the plastic deformation will be remained on the surface of the material to form an indentation. Figures 1 and 2 show the typical nanoindentation load-displacement curves and indentation profiles. We identify indentation depths: h_f, h_s, h_c for the depth of indentation after unloading, the displacement of the surface at the perimeter and the maximum contact depth, respectively. It can be concluded that

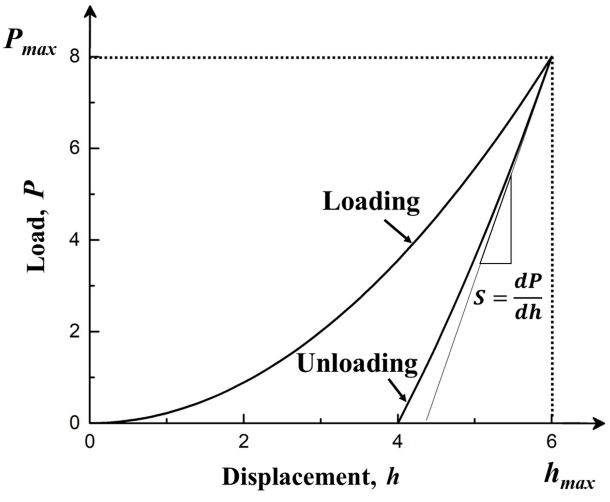

Figure 1: Typical load-displacement curve

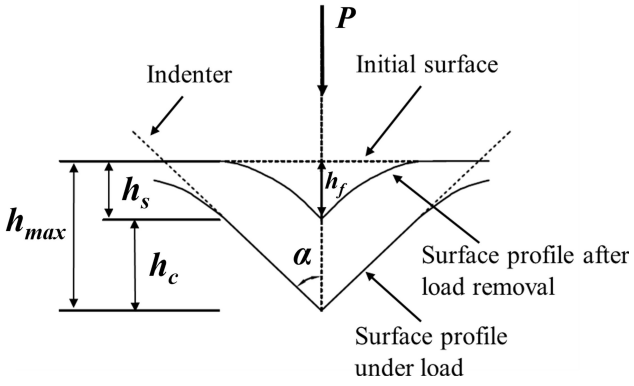

Figure 2: Schematic diagram of parameters after unloading

$h_{\max} = h_c + h_s$. The contact area of a perfect Berkovich indenter can be computed as a function of h_c as $A_c = 24.5h_c^2$.

When calculating elastic modulus and hardness by Oliver&Pharr method, the hardness (H) and equivalent modulus (E_r) can be defined by the following formula

$$H = \frac{P_{\max}}{A_c} \tag{1}$$

$$E_r = \frac{S\sqrt{\pi}}{2\beta\sqrt{A_c}} \tag{2}$$

where $P_{\max}$ is the maximum loading load and β is the parameter related to the shape of the indenter. For the Berkovich indenter, the value of β is 1.14 [33]. The slope $S = \mathrm{d}P/\mathrm{d}h$ can be computed from the first 60% span of the unloading curve as shown in Figure 1. The elastic modulus of the tested material, E, can be related to the equivalent modulus using

$$\frac{1}{E_r} = \frac{1-\nu^2}{E} + \frac{1-\nu_i^2}{E_i} \tag{3}$$

where E_i and ν_i are the elastic modulus and Poisson's ratio of the indenter material, respectively. For diamond indenter, $E_i = 1141$ GPa, $\nu_i = 0.07$ (given by equipment parameters). ν is the Poisson's ratio of the sample, which is assumed to be 0.38 (measured by tensile experiments).

When the Berkovich indenter is selected to indent the specimen under constant load, the creep compliance, $J(t)$, can be obtained from the following formula [34]

$$J(t) = \frac{4tan\alpha \cdot h^2(t)}{\pi(1-\nu)P_{\max}} \tag{4}$$

where $h(t)$ is the indentation depth, α is the half cone angle of Berkovich indenter while $\alpha = 70.3^\circ$ and t is the holding time of the maximum load. The shear creep compliance of the coating can be determined by fitting the experimental data in the holding stage.

3 Experimental

3.1 Materials and sample preparation

The experimental materials, epoxy resin (E-44) and curing agent, were purchased from Shanghai Youfu adhesive Co., Ltd. Ethanol and acetone were purchased from Chinese Medicines holding Chemical Reagent Co., Ltd. The molybdenum disulfide (MoS_2) powders and carbon nanofibers-molybdenum disulfide (CNF-MoS_2) powders were fabricated according to the reference [35]. A one-step hydrothermal method was used and then the MoS_2 nanosheets were in-situ prepared on CNF surface. Transfer the mixed solution to a Teflon-lined autoclave (50 mL), and placed in an electric oven with 210°C for 24 h. The as-prepared product was naturally cooled to room temperature, and then washed by distilled water and ethanol several times and dried overnight. The CNF/MoS_2 core-shell hybrid was acquired.

The EP/CNF-MoS_2 composite coatings were acquired as follows. Firstly, the CNF-MoS_2 powders were predispersed in the mixture solution of acetone and ethanol (1:1 volume ratio). Then, the epoxy resin (EP) was dissolved in the solution which was stirred at room temperature for 1 h. Later, the curing agent was slowly added followed by continually stirring until uniform epoxy composite was formed. After that, 45-steel disks (φ 18mm × 3mm) were polished with waterproof sandpaper and cleaned by ultrasonic for 10 minutes. The steel disks were uniformly coated with the prepared epoxy composites with air spraying process at room temperature and 50-55% relative air humidity. After evaporation of solvent and solidification at 100°C for 2 h, the polymer coating was finally obtained. Coatings with Pure-EP and EP/MoS_2 were prepared by the same method as samples for comparison. The images of the three coating specimens are shown in Figure 3.

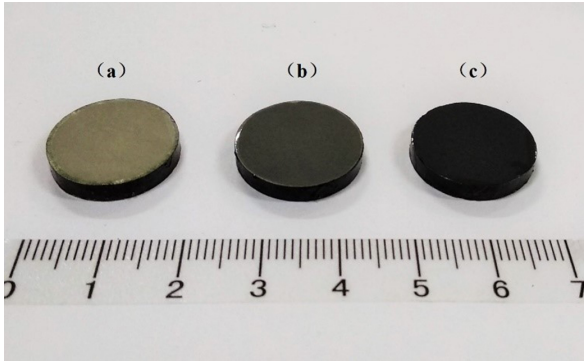

Figure 3: Image of coating specimens: a) Pure-EP; b) EP/ MoS_2; c) EP/CNF- MoS_2

3.2 Characterization

A transmission electron microscope (TEM, jeol-2010) and a field emission scanning electron microscope (SEM, 7800F) with an energy-dispersive X-ray spectrometer (EDS) were used to characterize the morphology and microstructure. The indentation tests were conducted using the Nano Indenter G200 (USA). The maximum applied load of the instrument is 500 mN, the resolution of the load is 50 nN, the maximum indentation depth is 500 μm, and the resolution of displacement is 0.01 nm.

The coating samples that have been sprayed with Pure-EP, EP/ MoS_2, and EP/CNF-MoS_2 were polished before the indentation tests. The Berkovich indenter was selected, and the curvature radius (a) of the indenter was 20 nm. Load control mode was adopted for all loading points. In order to avoid matrix effect when indentation depth is too deep on a coating film, the '1/10 rule of thumb' is often used, *i.e.* the measured mechanical parameter has its true value when indentation depth is less than 1/10 of the film thickness [32]. After tentative indentations, the maximum indentation load was selected to be 8 mN. Then, four loading conditions with a magnitude of 1, 2, 3 and 4 mN were mainly implemented in the experiments. The loading rate was 0.08 mN/s, the hold time of peak loading was 60 s and the unloading was at the same rate until the indenter had no contact with the specimen. Three tests were performed for each load control mode, and the results were averaged as the output experimental data. A total of 12 points were selected on the surface of each sample for indentation, and each indentation point interval was greater than 3 times the diameter of the indenter to avoid the mutual interference of each indentation point.

4 Results and discussion

4.1 Microstructure

Figure 4 shows the optical microscope image of the cross-section of the EP/CNF-MoS_2 coating specimen. Clearly, the coating thickness is uniformly distributed with an average of 47 μm. The thickness of the other two kinds of coating specimen is similar since the fabricating process was the same. The microstructure of the original CNF-MoS_2 hybrid material is shown in Figure 5a. It can be seen that the average diameter of the CNFs is 100 nm and each CNF is uniformly wrapped up with MoS_2 nano-sheets (200-300 nm), which is similar to silk ribbons on a rope. Figure 5b shows a single CNF-MoS_2 hybrid material in the coating, which indicates that it has a strong bonding with the epoxy resin matrix. A rectangle area on the coating surface was selected for EDS element mapping as shown in Figure 5c. The results of the element mapping are shown in Figure 5d-5f), in which carbon accounted for 97% of the total elements, sulfur and molybdenum accounted for 2% and 1%, respectively. The results show that nanomaterials are generally well dispersed in the matrix, and the agglomeration of nanofillers is not formed. The good dispersion of nanomaterials in epoxy resin ensures the representativeness and repeatability of the indentation test data.

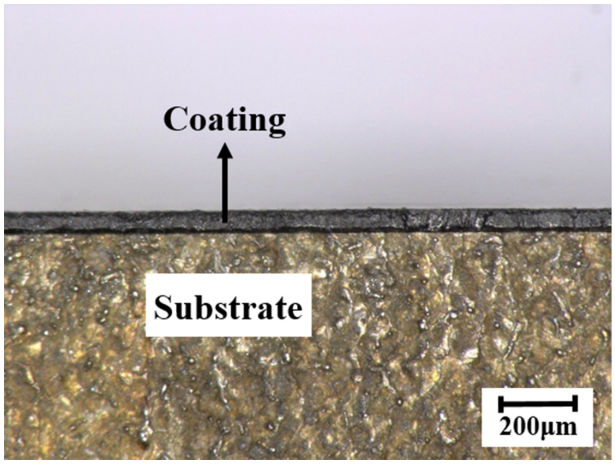

Figure 4: Microscope image of a cross-section of the EP/CNF-MoS_2 specimen

4.2 Nanoindentation test

4.2.1 Load-displacement curve

As an example, typical load-displacement curves of EP/CNF-MoS_2 specimen measured by nanoindentation at different indentation points are shown in Figure 6, the maximum indentation load is 3 mN. The indentation curve can be divided into three stages, namely, loading stage, holding stage, and unloading stage. The maximum indentation depth of the four indentation experiments ranged from 1641 to 1787 nm, and the displacement at the holding stage ranged from 250 to 330 nm. It can be seen that the load-displacement curves at different indentation points show good consistency in three stages, which indicates that the properties of the coating are uniform and the indentation test is repeatable.

Typical load-displacement curves of specimens with different components under 1, 2, 3 and 4 mN are plot-

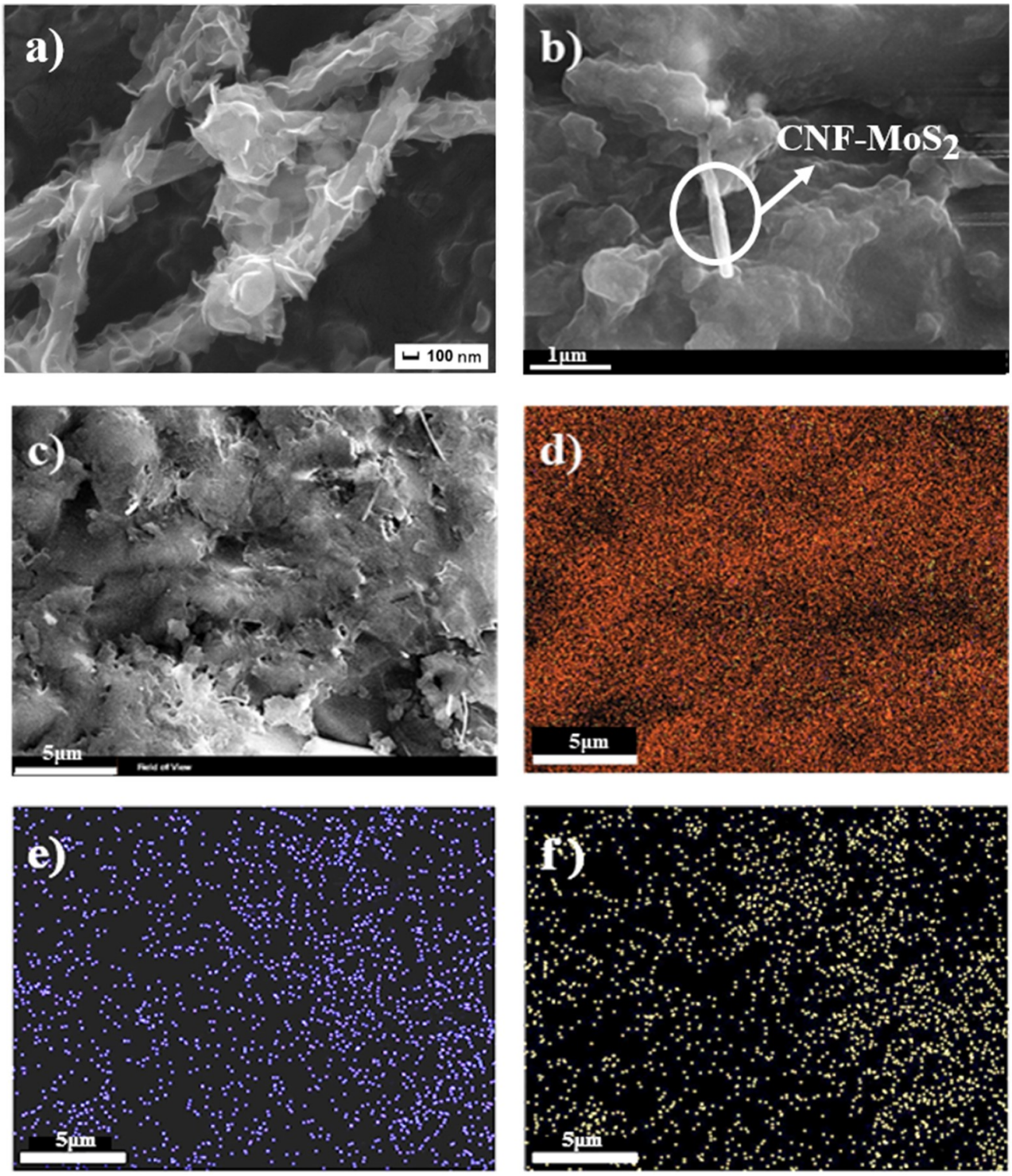

Figure 5: Microstructure of EP/CNF-MoS_2: a) TEM image of CNF-MoS_2, MoS_2 nano-sheets are uniformly coated on the surface of CNFs; b) SEM image of a single CNF-MoS_2 hybrid in the coating; c) A rectangle area selected for EDS composition scanning; d), e), and f) are the results of the EDS composition scanning; d) Total components including C, Mo and S; e) Mo; f) S

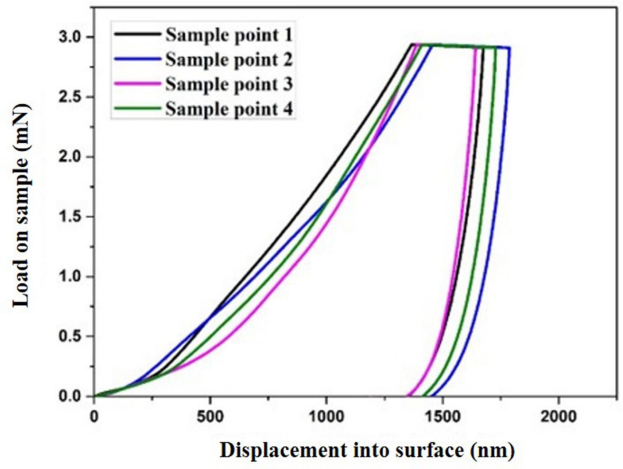

Figure 6: Typical load-displacement curves of EP/CNF-MoS_2 specimen (the maximum indentation load is 3mN)

ted in Figure 7. In the loading stage, the indentation displacement of the specimen with MoS_2 particles is relatively smaller than that of the pure epoxy specimen at the same loading magnitude; the indentation displacement of the specimen with nano-hybrid particles is the smallest one among the three loading curves. In the peak-load holding stage, the maximum loads of the three specimens are same at each loading condition and a platform of each curve is shown after 60 s holding time. In the unloading stage, the indentation displacement of each test decreases gradually when the load turns to be zero.

The total indentation depth in the loading stage were investigated as shown in Figure 8. It can be seen that the indentation depth of the MoS_2 coating decreases about 18% compared with the EP coating and the indentation depth of CNF-MoS_2 hybrid coating decreases by about 28% compared with the MoS_2 coating. The results demonstrate that the incorporation of nano-particles improves the bearing capacity of the EP material, also the incorporation of CNFs additionally improves the bearing capacity of the EP/MoS_2 composites.

Additionally, the maximum indentation depth of the EP material at the indentation load of 4 mN is about 3.5 μm, which is less than 1/10 of the coating thickness (about 4.7 μm). It should be pointed out that failure occurs when the indentation load is larger than 4 mN due to the abnormal unloading data in the tests. Thus, the maximum indentation load for the EP coating is 4 mN. However, the maximum indentation load can reach 6 mN for the MoS_2 coating and 8 mN for the CNF-MoS_2 hybrid coating due to smaller indentation displacement at the same load.

4.2.2 Elastic modulus and hardness

Elastic modulus (E) and the hardness (H) are calculated based on Eqs. (1)-(3) according to the unloading stage in Figure 7. Figure 9 is a histogram of material parameters of epoxy resin and its composites under different indentation loads. As Figure 9a shown, the elastic modulus of each specimen under different loads increases with the increasing indentation load. The elastic modulus of epoxy resin specimens with nanoparticles is generally higher than that of pure epoxy resin specimens, and the increase of the elastic modulus of EP/CNF-MoS_2 nanohybrid material is significantly larger than the other two. Figure 9b shows the hardness changes of three kinds of specimens under different indentation loads. General speaking, the hardness values of EP/CNF-MoS_2 nanohybrid composite are greater than those of the other two materials. This is mainly due to the superior hardness characteristics of CNF. Thus, it can be concluded that the addition of CNF makes the load-bearing capacity of EP/CNF-MoS_2 significantly higher than that of Pure-EP and EP/MoS_2 materials.

Figure 10 shows the variation of E and H at different indentation loads. As we can see that the magnitude of E of each specimen keeps almost constant when the indentation load is not greater than 3 mN, while it changes significantly when the indentation load is greater than 3 mN. It should be pointed out that the main reason for different modulus values among 1~3 mN is the spraying method. The coating is made of multi-layer spraying, this method will often produce tiny holes in the film, so the density of the film is poor when the indentation depth is small, which will lead to the measured elastic modulus is small, with the increase of the indentation load, the density of the film in contact with the indenter gradually improved, the value gradually increased and close to the true value of the material. Additionally, the magnitude of H of each specimen keeps almost constant at different indentation load. Reasonably, in order to eliminate the measurement errors, the elastic modulus and hardness obtained at the indentation load of 3 mN are selected for comparison of different coating specimens.

The average values of E and H of different materials under the maximum load of 3 mN were extracted. As Table 1 shown, compared with the EP coating, the elastic modulus, and hardness of MoS_2 coating increase 26% and 37%, respectively, while the elastic modulus and hardness of CNF-MoS_2 hybrid coating increase 47.8% and 104.3%, respectively. The results indicate that the mechanical properties including elastic modulus and hardness have been significantly improved after adding CNF-MoS_2 hybrids into the epoxy resin coating.

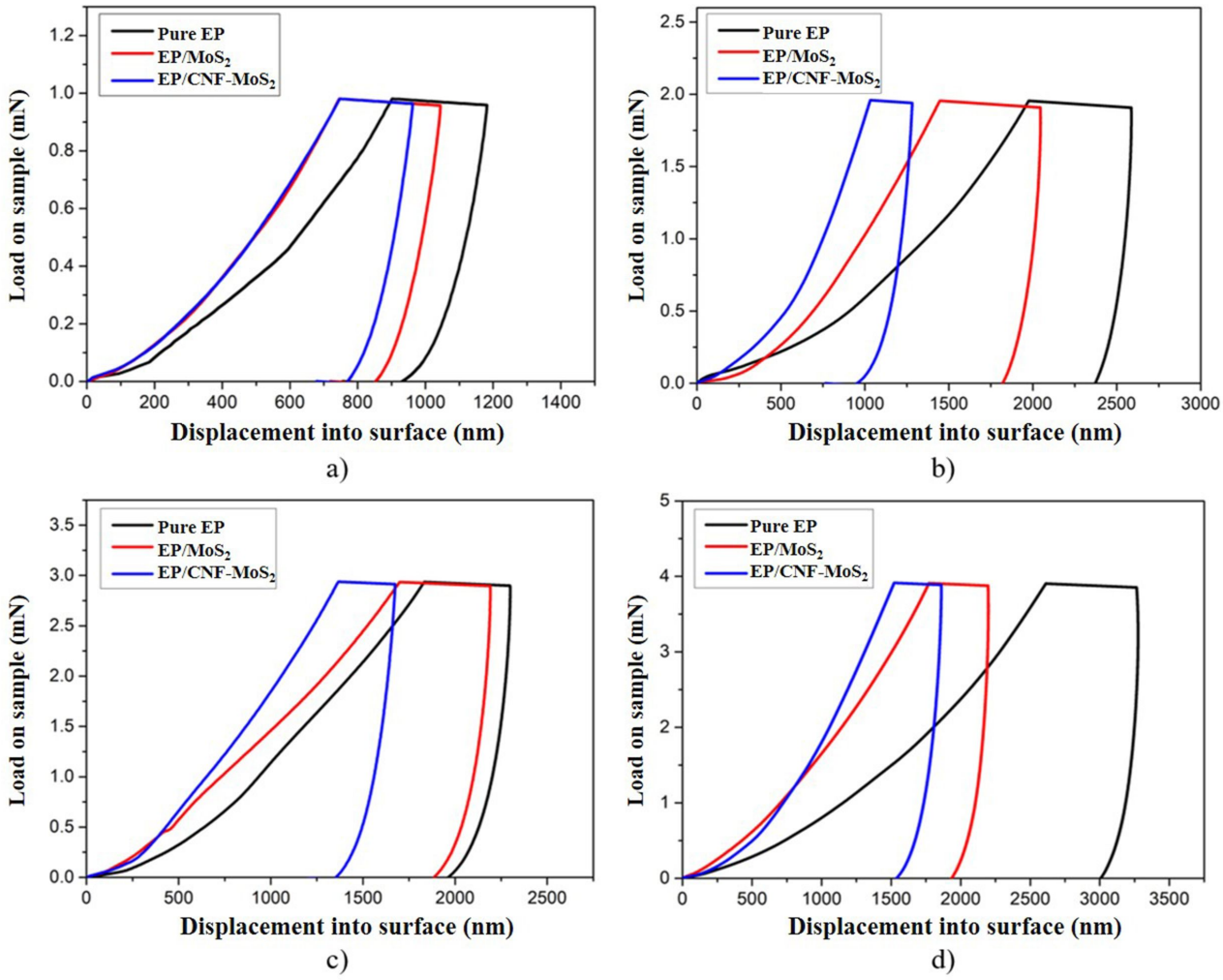

Figure 7: Load-displacement curves under different maximum loading loads: a) 1 mN; b) 2 mN; c) 3 mN; d) 4 mN

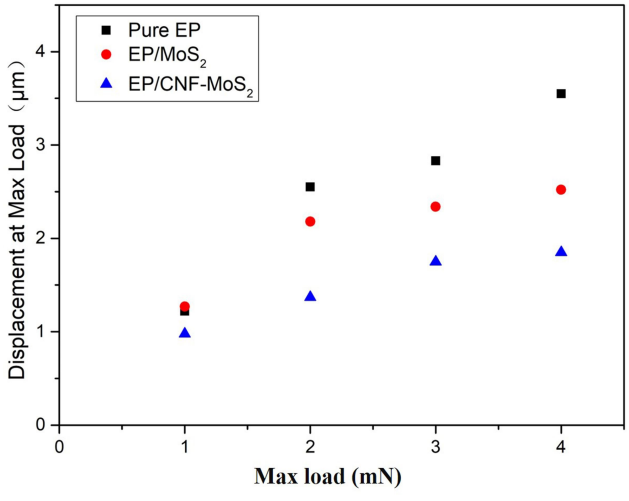

Figure 8: Variation of indentation depths at maximum load in end of the loading stage

Table 1: Average *E* and *H* of coating specimens at an indentation load of 3 mN

Coating sample	*E* (GPa)	Increased magnitude	*H* (MPa)	Increased magnitude
Pure-EP	1.9		23	
EP/MoS_2	2.4	26%	34	47.8%
EP/CNF-MoS_2	2.6	37%	47	104.3%

4.2.3 Creep properties

The indentation depth varies with the holding time in the holding stage, which can be used to explore the creep property of the coating material. Figure 11 shows the variation of depth, or the creep displacement, with the holding time under different maximum load. The total creep displacement of the epoxy resin is larger than those incorporated with nano-particle fillers in the entire holding

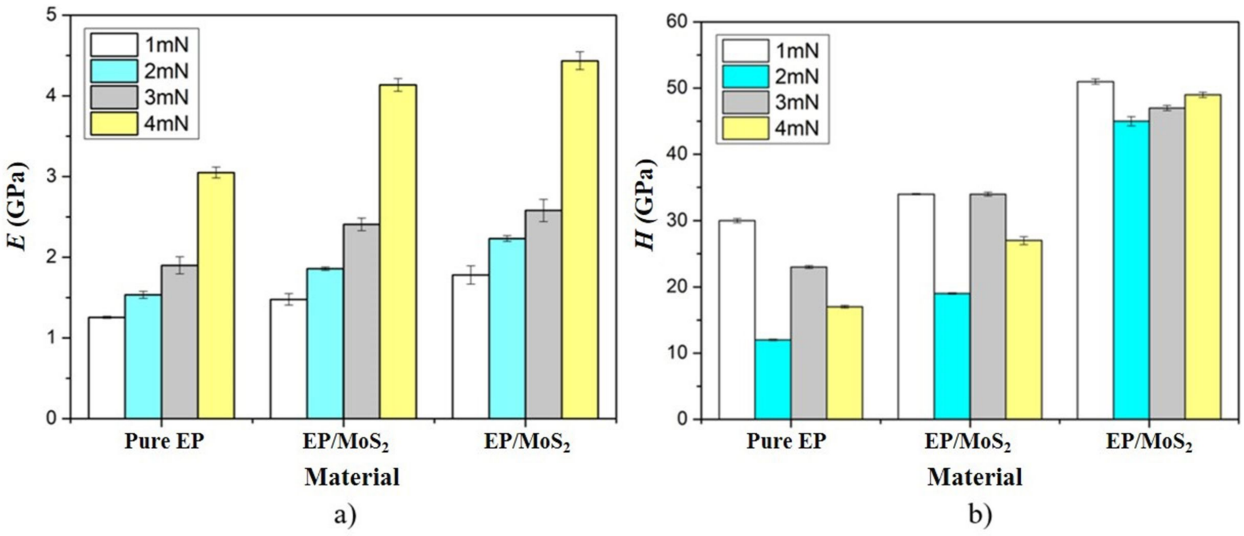

Figure 9: Histograms of a) elastic modulus; b) hardness under different indentation loads

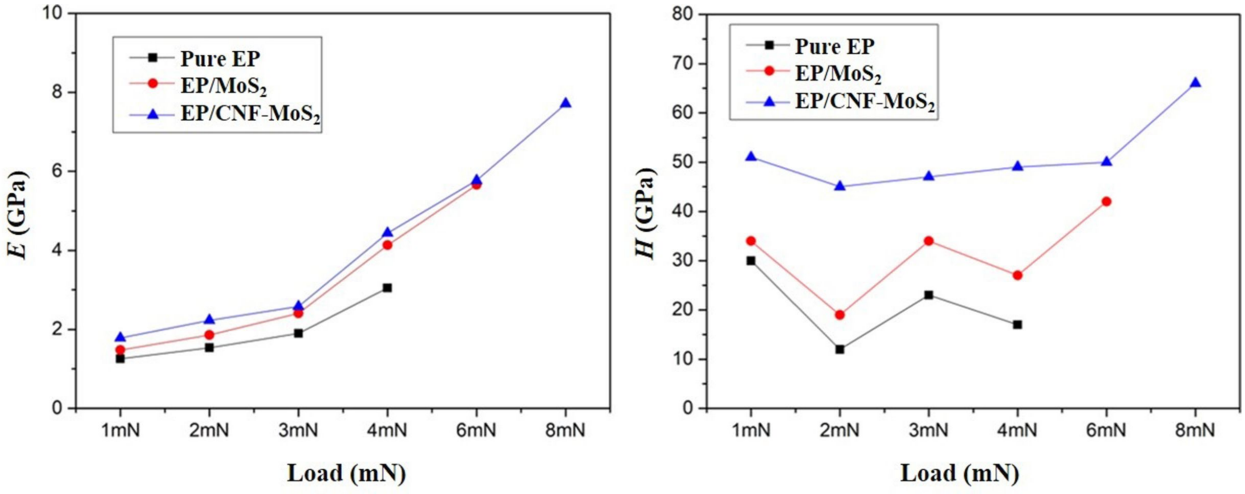

Figure 10: Variation of *E* and *H* at different indentation loads

stage. Furthermore, the creep displacement of the CNF-MoS_2 nanohybrid material is much less than that of the MoS_2 coating material and its curve with the holding time grows smoother than that of the MoS_2 coating material. The total creep displacement of different materials with the maximum load is shown in Figure 12. The creep displacement of EP/CNF-MoS_2 is significantly smaller than that of EP and EP-MoS_2 coatings under different maximum indentation loads, and the creep displacement reduction effect is more obvious when the indentation load is 2 mN and 3 mN. The results demonstrate that the creep resistance of the epoxy resin composite coating with CNF-MoS_2 fillers has been significantly improved.

According to Eq. (3), the shear creep compliance of the coating specimens can obtained based on the variation of depth with holding time under different maximum load in the holding stage. Figure 13 shows the creep compliance curves of the three different polymer coating specimens, which have the same tendency with Figure 11. Table 2 shows the average creep compliance of the coating specimens under different maximum load in the holding

Table 2: Average creep compliance of coating specimens under different maximum load in the holding stage

Coating sample	1 mN	2 mN	3 mN	4 mN	Average
Pure-EP	1.29	4.36	6.08	7.54	4.82
EP/MoS_2	1.02	3.61	4.19	7.08	3.98
EP/CNF-MoS_2	0.72	1.55	2.68	2.97	1.98

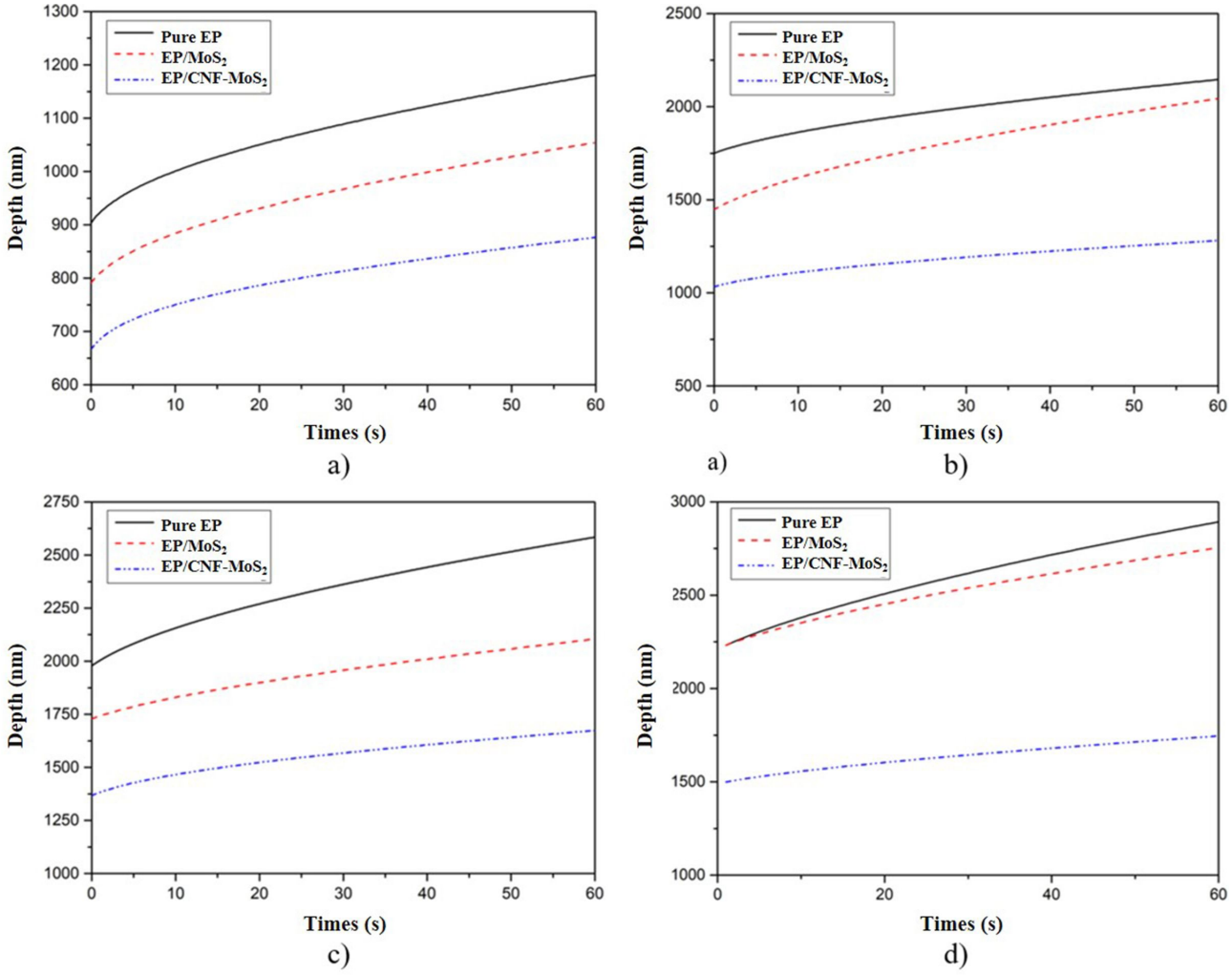

Figure 11: Variation of depth with holding time under different maximum load in the holding stage: a) 1 mN; b) 2 mN; c) 3 mN; d) 4 mN

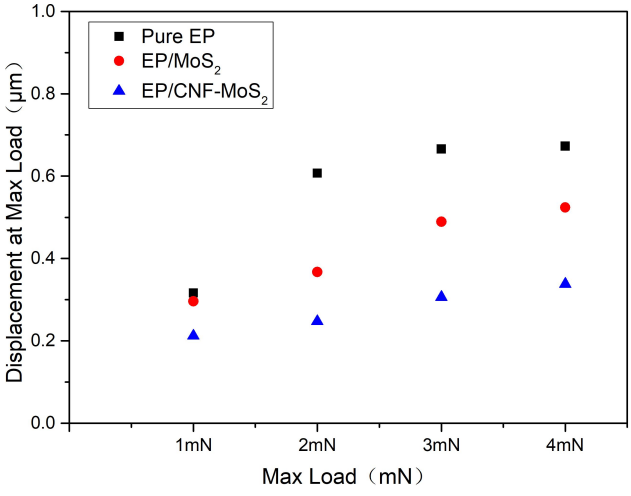

Figure 12: Total creep displacement of different materials at different max load in the holding stage

stage, and the value of Pure-EP, EP/MoS_2, and EP/CNF-MoS_2 is 4.82, 3.98, and 1.98, respectively. Apparently, the addition of CNF-MoS_2 nanohybrid particles can effectively improve the creep deformation resistance of epoxy resin composite coatings.

4.2.4 Discussion

According to the microstructure analysis of epoxy coatings modified by CNF-MoS_2 nanoparticles, a schematic diagram of CNF-MoS_2 nanohybrid composites is illustrated as shown in Figure 14. It can be seen that the wrapped structure is formed when MoS_2 sheets grown on the surface of each CNF. The nanohybrid structure can not only improve the dispersion of MoS_2 in the epoxy matrix, but also increase the specific surface area of the nanoparticles. The incorporation of the nanohybrid material in the epoxy

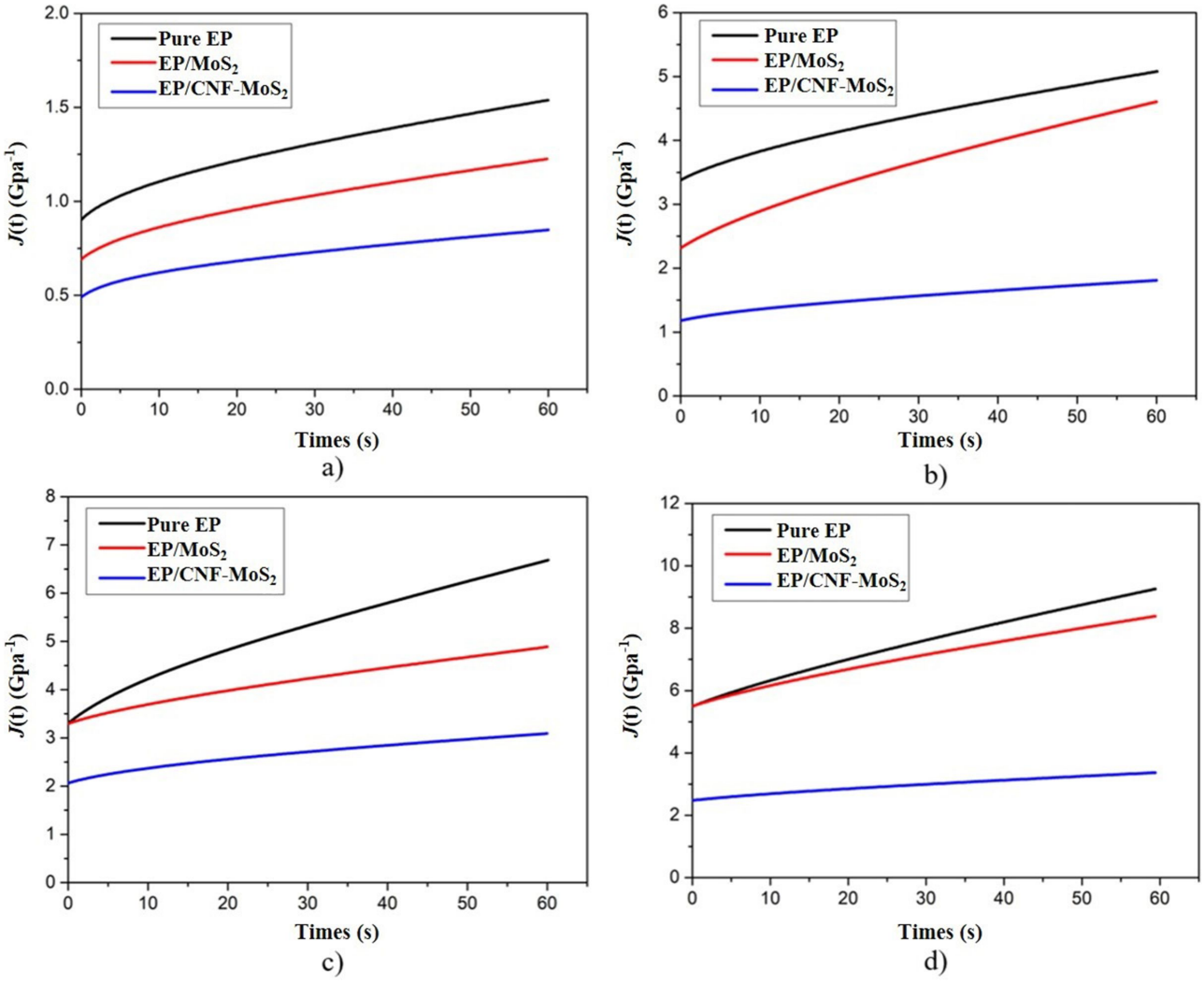

Figure 13: Creep compliance of coating specimens under different maximum load in the holding stage: a) 1 mN; b) 2 mN; c) 3 mN; d) 4 mN

matrix can form a three-dimensional structure. As a result, the epoxy matrix can transfer the stresses to CNF-MoS_2 nanohybrids in the working area under the indenter when the coating is subjected to the external force, which can subsequently improve the bearing capacity, elastic modulus and creep stiffness of the nanohybrid composites.

The effects of Pure EP, EP/MoS_2 and EP/CNF-MoS_2 coating specimens on the friction and wear properties are shown in Figure 15 [15]. Compared with the Pure EP specimen, the friction coefficient and wear rate of the EP-MoS_2 coating decrease by 78% and 76%, respectively. Furthermore, compared with the EP-MoS_2 coating, the wear rate of the EP/CNF-MoS_2 coating decreases by 49%, while the friction coefficient of the EP/CNF-MoS_2 coating remains almost same. The indentation results obtained by nanoindentation test can further reveal the improvement mechanism of CNF-MoS_2 nanohybrid materials on the tribological properties of epoxy resin coatings. When MoS_2 nanosheets grow on the surface of CNFs, the wrapping structure is formed, which can improve the dispersion of MoS_2 in the epoxy matrix and increase the specific surface area of nanoparticles. As a result, the hybrid nanoparticles can increase the contact area and reduce the friction coefficient of composite coatings. In addition, the hardness of the EP/CNF-MoS_2 coating deserves to be greatly improved due to the superior high hardness of CNFs, so the wear resistance of the coating material is greatly improved and the wear rate is significantly reduced. Generally, the CNF-MoS_2 nanohybrid materials show comprehensive friction properties with better lubrication performance as well as low wear rate.

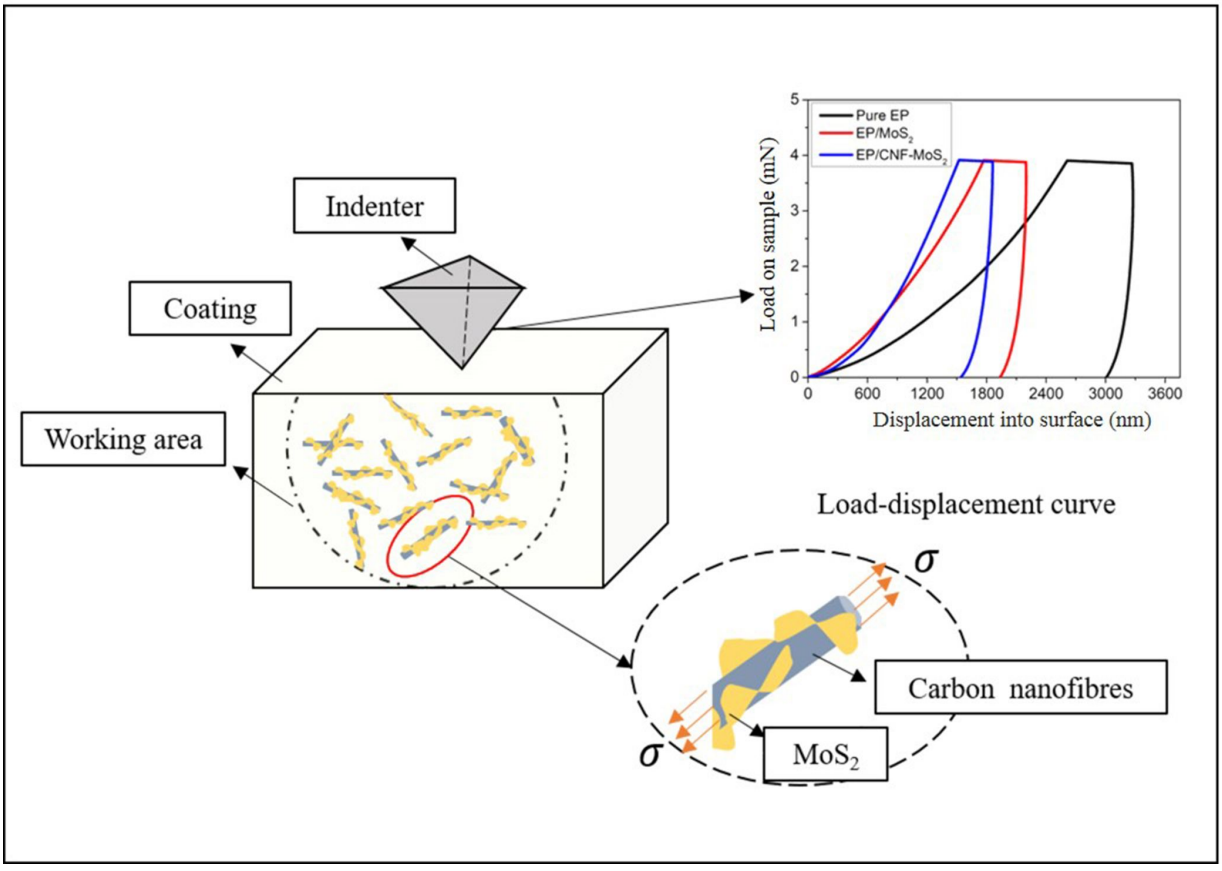

Figure 14: Schematic illustration of the indentation process of EP/CNF-MoS_2 composites

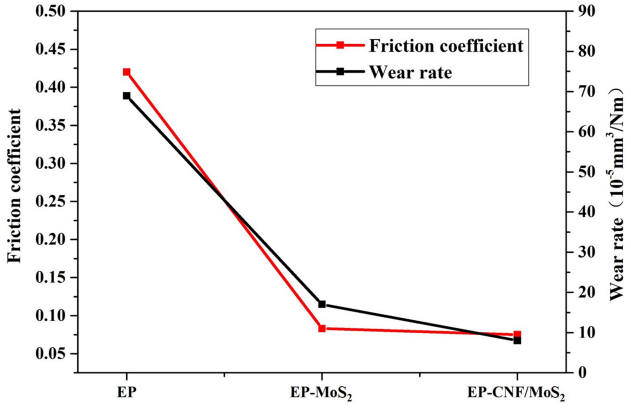

Figure 15: Variation of friction coefficient and wear rate of coating specimens

5 Conclusions

In this paper, a CNF-MoS_2 nanohybrid material was prepared and incorporated into epoxy resin to fabricate an EP/CNF-MoS_2 coating material. The results of microstructure and composition characterization show that nanomaterials are generally well dispersed in the matrix, without agglomeration.

Nanoindentation experiments were carried out on samples with the EP/CNF-MoS_2 coatings on 45 steel substrates to further explore the effect of CNF-MoS_2 nanohybrid materials on the mechanical properties of epoxy resin coatings. The elastic modulus of EP/CNF-MoS_2 coating increases by 37% and 26% compared with the Pure-EP and EP/MoS_2, respectively. The hardness of EP/CNF-MoS_2 coating increases 104.3% and 47.8% compared with the Pure-EP and EP/MoS_2, respectively. The average creep compliance of the EP/CNF-MoS_2 coating decreases 58.9% and 50.3% compared with the Pure-EP and EP/MoS_2, respectively. The indentation results have demonstrated that the EP/CNF-MoS_2 coating shows much better mechanical properties, and its elastic modulus, hardness and creep property have been greatly improved.

The improved tribological performance of epoxy resin coatings by incorporation of CNF-MoS_2 nanohybrid fillers can be explained by the mechanical tests using the nanoindentation. It can be concluded that the wrapping structure with MoS_2 nano-sheets growing on the surface of CNFs

increases the contact area and reduces the friction coefficient of composite coatings, while the wear resistance of the coating material is also greatly improved due to the superior high hardness of CNFs.

Acknowledgement: The authors are grateful for the financial support from the National Natural Science Foundation of China (Grant Nos. 11672345,11972014), the Natural Science Foundation of Jiangsu Province (Grant Nos. BK20150479) and the Six Talent Peaks Project in Jiangsu Province (Grant No.2016-HKHT-004)

References

[1] Boumaza M., Khan R., Zahrani S., An experimental investigation of the effects of nanoparticles on the mechanical properties of epoxy coating, Thin Solid Films., 2016, 620, 160-164.
[2] Palraj S., Selvaraj M., Maruthan K., Rajagopal G., Corrosion and wear resistance behavior of nano-silica epoxy composite coatings, Prog. Org. Coatings., 2015, 81, 132-139.
[3] Wan Q., Jin Y., Sun P., Ding Y., Rheological and tribological behaviour of lubricating oils containing platelet MoS_2 nanoparticles, J. Nanoparticle Res., 2014, 16, 2386.
[4] Rajendhran N., Palanisamy S., Periyasamy P., Venkatachalam R., Enhancing of the tribological characteristics of the lubricant oils using Ni-promoted MoS_2 nanosheets as nano-additives, Tribol. Int., 2018, 118, 314-328.
[5] Xu Y., Hu K., Jiang Y., Sun X., Hu X., Tribology of MoS_2-Based Nanocomposites, Tribol. of Nanocomposites., Springer Berlin Heidelberg, 2012.
[6] Xu Z.Y., Xu Y., Hu K.H., Xu Y.F., Hu X.G., Formation and tribological properties of hollow sphere-like nano-MoS_2 precipitated in TiO_2 particles, Tribol. Int., 2015, 81, 139-148.
[7] Hou K., Wang J., Yang Z., Ma L., Wang Z., Yang S., One-pot synthesis of reduced graphene oxide/molybdenum disulfide heterostructures with intrinsic incommensurateness for enhanced lubricating properties, Carbon N. Y., 2017, 115, 83-94.
[8] Zhang Y., Park S.J., Imidazolium-optimized conductive interfaces in multilayer graphene nanoplatelet/epoxy composites for thermal management applications and electroactive devices, Polymer (Guildf) ., 2019, 168, 53-60.
[9] Zhang Y., Park S.J., Influence of the nanoscaled hybrid based on nanodiamond@graphene oxide architecture on the rheological and thermo-physical performances of carboxylated-polymeric composites, Compos. Part A Appl. Sci. Manuf., 2018, 112, 356-64.
[10] Peng Y., Hu X., Zheng X., Olson D., Xu Y., Geng J., Tribological behavior of Fe_3O_4/MoS_2 nanocomposites additives in aqueous and oil phase media, Tribol. Int., 2016, 102, 79-87.
[11] Alazemi A.A., Dysart A.D., Phuah X.L., Pol V.G., Sadeghi F., MoS_2 nanolayer coated carbon spheres as an oil additive for enhanced tribological performance, Carbon N. Y., 2016, 110, 367-77.
[12] Chen B., Li X., Jia Y., Li X., Yang J., Yan F., et al., MoS_2 nanosheets-decorated carbon fiber hybrid for improving the friction and wear properties of polyimide composite, Compos. Part A Appl. Sci. Manuf., 2018, 109, 232-8.
[13] Al-Saleh M.H., Sundararaj U., A review of vapor grown carbon nanofiber/polymer conductive composites, Carbon N. Y., 2009, 47, 2-22.
[14] Taheri-Behrooz F., Esmkhani M., Yaghoobi-Chatroodi A., Ghoreishi S.M., Out-of-plane shear properties of glass/epoxy composites enhanced with carbon-nanofibers, Polym. Test., 2016, 55, 278-86.
[15] Chen B., Jia Y., Zhang M., Liang H., Li X., Yang J., et al., Tribological properties of epoxy lubricating composite coatings reinforced with core-shell structure of CNF/MoS_2 hybrid, Compos. Part A Appl. Sci. Manuf., 2019, 122, 85-95.
[16] Li X., Bhushan B., A review of nanoindentation continuous stiffness measurement technique and its applications, Mater. Charact., 2002, 48, 11-36.
[17] Poon B., Rittel D., Ravichandran G., An analysis of nanoindentation in linearly elastic solids, Int. J. Solids Struct., 2008, 45, 6018-6033.
[18] Oliver W.C., Pharr G. M., An improved technique for determining hardness and elastic modulus using load and displacement sensing indentation experiments, J. Mater. Res., 1992, 7, 1564-83.
[19] Hodzic A., Stachurski Z.H., Kim J.K., Nano-indentation of polymer-glass interfaces. Part I. Experimental and mechanical analysis, Polymer (Guildf)., 2000, 41, 6895-6905.
[20] Hodzic A., Stachurski Z.H., Kim J.K., Nano-indentation and nano-scratch of polymer/glass interfaces. II: Model of interphases in water aged composite materials, Polymer (Guildf)., 2001, 42, 5701-10.
[21] Shen L., Phang I.Y., Liu T., Zeng K., Nanoindentation and morphological studies on nylon 66/organoclay nanocomposites. II. Effect of strain rate, Polymer (Guildf)., 2004, 45, 8221-9.
[22] Liu T., Phang I.Y., Shen L., Chow S.Y., Zhang W. De., Morphology and mechanical properties of multiwalled carbon nanotubes reinforced nylon-6 composites, Macromolecules., 2004, 37, 7214-22.
[23] Shen L., Phang I.Y., Chen L., Liu T., Zeng K., Nanoindentation and morphological studies on nylon 66 nanocomposites. I. Effect of clay loading, Polymer (Guildf)., 2004, 45, 3341-3349.
[24] Shen L., Tjiu W.C., Liu T., Nanoindentation and morphological studies on injection-molded nylon-6 nanocomposites, Polymer (Guildf)., 2005, 46, 11969-11977.
[25] Lee S.H., Wang S., Pharr G.M., Xu H., Evaluation of interphase properties in a cellulose fiber-reinforced polypropylene composite by nanoindentation and finite element analysis, Compos. Part A Appl. Sci. Manuf., 2007, 38, 1517-1524.
[26] Melgarejo Z.H., Resto P.J., Stone D.S., Suárez O.M., Study of particle-matrix interaction in Al/AlB_2 composite via nanoindentation, Mater. Charact., 2010, 61, 135-40.
[27] Sánchez M., Rams J., Campo M., Jiménez-Suárez A., Ureña A., Characterization of carbon nanofiber/epoxy nanocomposites by the nanoindentation technique, Compos. Part B Eng., 2011, 42, 638-44.
[28] Kavouras P., Dragatogiannis D.A., Batsouli D.I., Charitidis C.A., Effect of local microstructure on the indentation induced damage of a fiber reinforced composite, Polym. Test., 2017, 61, 197-204.
[29] Tehrani M., Safdari M., Al-Haik M.S., Nanocharacterization of creep behavior of multiwall carbon nanotubes/epoxy nanocomposite, Int. J. Plast., 2011, 27, 887-901.
[30] Hou X.D., Jennett N.M., Defining the limits to long-term nanoindentation creep measurement of viscoelastic materials, Polym. Test., 2018, 70, 297-309.

[31] Koumoulos E.P., Jagadale P., Lorenzi A., Tagliaferro A., Charitidis C.A., Evaluation of surface properties of epoxy-nanodiamonds composites, Compos. Part B Eng., 2015, 80, 27-36.
[32] Mishra K., Singh R.P., Quantitative evaluation of the effect of dispersion techniques on the mechanical properties of polyhedral oligomeric silsesquioxane (POSS)-epoxy nanocomposites, Polym. Compos., 2018, 39, E2445-53.
[33] Oliver W., Pharr G., Measurement of hardness and elastic modulus by instrumented indentation: Advances in understanding and refinements to methodology, J. Mater. Res., 2004, 19, 3-20.
[34] Peng G., Ma Y., Feng Y., Huan Y., Qin C., Zhang T., Nanoindentation creep of nonlinear viscoelastic polypropylene, Polym. Test., 2015, 43, 38-43.
[35] Chen B., Jia Y., Zhang M., Liang H., Li X., Yang J., et al., Tribological properties of epoxy lubricating composite coatings reinforced with core-shell structure of CNF/MoS_2 hybrid, Compos. Part A Appl. Sci. Manuf., 2019, 122, 85-95.